Preprint Title Azologization of a hetero-stilbene based c-RAF kinase inhibitor: Towards the design of photoswitchable sirtuin inhibitors

Authors Christoph W. Grathwol, Nathalie Wössner, Sören Swyter, Adam C. Smith, Enrico Tapavicza, Robert K. Hofstetter, Anja Bodtke, Manfred Jung and Andreas Link

Article Type Full Research Paper

Supporting Information File 1 Supp1.docx; 54.8 MB

ORCID® iDs Christoph W. Grathwol - https://orcid.org/0000-0003-0232-3279; Enrico Tapavicza - https://orcid.org/0000-0002-0640-0297; Robert K. Hofstetter - https://orcid.org/0000-0002-1077-9703; Andreas Link - https://orcid.org/0000-0003-1262-6636

Azologization of a hetero-stilbene based c-RAF kinase inhibitor: Towards the design of photoswitchable sirtuin inhibitors

Christoph W. Grathwol[1], Nathalie Wössner[2], Sören Swyter[2], Adam C. Smith[3], Enrico Tapavicza[3], Robert Hofstetter[1], Anja Bodtke[1], Manfred Jung[2] and Andreas Link*[1]

Address:

[1]Institute of Pharmacy, University of Greifswald, Friedrich-Ludwig-Jahn-Str. 17, 17489 Greifswald, Germany

[2]Institute of Pharmaceutical Sciences, University of Freiburg, Albertstr. 25, 79104 Freiburg, Germany

[3]Department of Chemistry and Biochemistry, California State University Long Beach, 1250 Bellflower Boulevard, Long Beach, CA, 90840 USA

Email: Andreas Link – link@uni-greifswald.de

* Corresponding author

Abstract

The use of light as an external trigger to change ligand shape and as a result its bioactivity, allows the probing of pharmacologically relevant systems with spatiotemporal resolution. In this context, aromatic diazeno compounds are well suited for the design of photoswitchable ligands due to the long thermal relaxation half-lives of the photoinduced *Z* configuration, and tunability of the absorption wavelength λ_{max}. In search for sirtuin inhibitors, a hetero-stilbene lead resulting from the screening of a compound that was originally designed as kinase inhibitor, was remodelled to its diazeno analogue. By this azologization, the shape of the molecule was left unaltered whereas the photoswitching ability was improved. As anticipated, the highly analogous compound showed similar activity in its thermodynamically stable stretched-out *E* form. Irradiation of this isomer triggers isomerisation to the *Z* configuration with a bent geometry causing a considerably shorter end-to-end distance. The resulting affinity shifts are intended to enable real-time photomodulation of sirtuins in vitro.

Keywords

Azo compounds; epigenetics; photoswitch; sirtuins; stilbenes

Introduction

Sirtuins are protein deacylases that cleave off not only acetyl, but also other acyl groups from the ε-amino group of lysines in histones and many other substrate proteins. This class of lysine deacetylases (KDACs) is distinguished from others by

their dependence on the cosubstrate NAD^+. In mammalians, seven sirtuin isoforms have been identified to date [1]. These can be grouped into five classes (I, II, III, IV and V) according to their phylogenetic relationship [2]. The isoforms Sirt1, Sirt2 and Sirt3 originate from the same phylogenetic branch (class I), but differ in their subcellular localization. Although Sirt1 and Sirt2 were shown to shuttle between nucleus and cytoplasm in a cell-type and cell-cycle dependent manner, Sirt1 is mainly found in the nucleoplasm and Sirt2 in the cytoplasm [3–7]. Sirt3 primarily resides in the mitochondrion [8]. Facing the multitude of diseases that are associated with a dysregulation of sirtuin activity, they represent a promising target for pharmaceutical intervention. For example, selisistat (EX-527, **1**), a nanomolar and selective Sirt1 inhibitor, passed phase II clinical trials as a disease-modifying therapeutic for Huntington's disease (HD) and was acquainted by AOP Orphan Pharmaceuticals AG for phase III trials in 2017 [9, 10]. Its structure comprises a carboxamide moiety, which mimics the amide group of the endogenous pan-sirtuin inhibitor nicotinamide. Likewise Sirt2 inhibition was shown to have beneficial effects in animal and cell models of neurodegenerative diseases like HD and Parkinson's disease [11, 12]. Sirt3 activity recently was found to play an important role in cardiovascular diseases and extended ageing in humans [13–17]. Regarding tumorigenesis, the knowledge on the influence of sirtuins is inconsistent. Sirt1, Sirt2 and Sirt3 all have been reported to act either as tumor suppressors or promotors, depending on the particular cell type [1].

The approach to new chemotypes for sirtuin inhibition via known adenosine mimicking kinase inhibitors has already been fruitful in the past [18, 19]. Therefore, a focused kinase inhibitor library from GlaxoSmithKline was screened for biological activity on

human sirtuin isoforms Sirt1–Sirt3. Aza-stilbene derivative GW435821X (**2a**), initially published as c-RAF kinase inhibitor, was identified as a moderately active Sirt2 inhibitor with low selectivity [20, 21].

Stilbene motives are part of artificial and natural photoswitches [22]. Thus, **2a** abides a possible access to photoswitchable inhibitors that could be useful tools in the further investigation of the biochemistry and pharmacology of sirtuins.

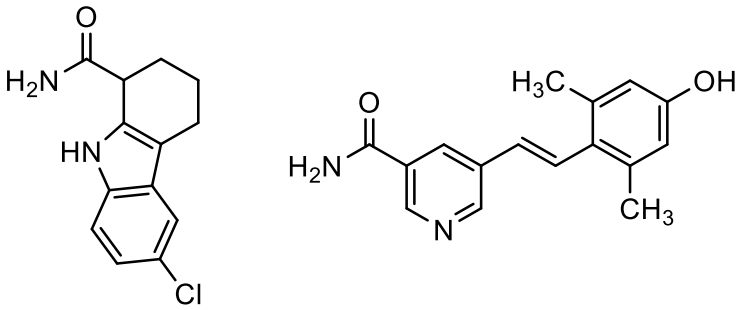

1 **2a**

Figure 1: Selisistat (**1**) and hit compound GW435821X (**2a**).

Results

Chemistry of Stilbenes

All stilbene derivatives were synthesised by palladium catalysed cross coupling reactions using either commercially available 5-bromonicotinamide (**3a**) or methyl 5-bromonicotinate (**3b**). If **3b** was used, transformation to the nicotinamide was accomplished almost quantitatively by addition of a saturated solution of ammonia in anhydrous methanol and stirring in a closed vessel at 40 °C. Compounds **4a** and **b** could easily be obtained through Suzuki coupling with commercially available

naphthalene-2-ylboronic acid or (3,4-dihydronaphthalen-2-yl)boronic acid (Scheme 1). The latter was synthesized according to a literature procedure [23].

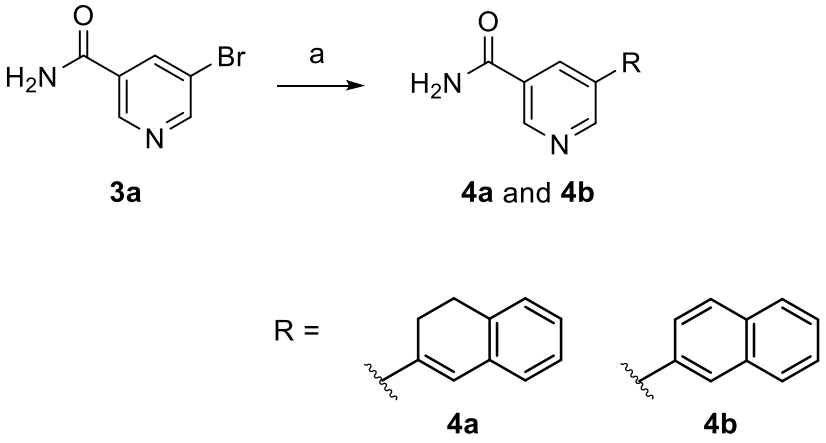

Scheme 1: Reagents and conditions: a) appropriate boronic acid, $Pd(PPh_3)_4$, Na_2CO_3, DMF, H_2O, microwave, 15 min, 150 °C, 43-64 %.

Formation of compounds **2b**-**h** was accomplished through Heck coupling of aryl bromides with the appropriate styrenes (Scheme 2) [24].

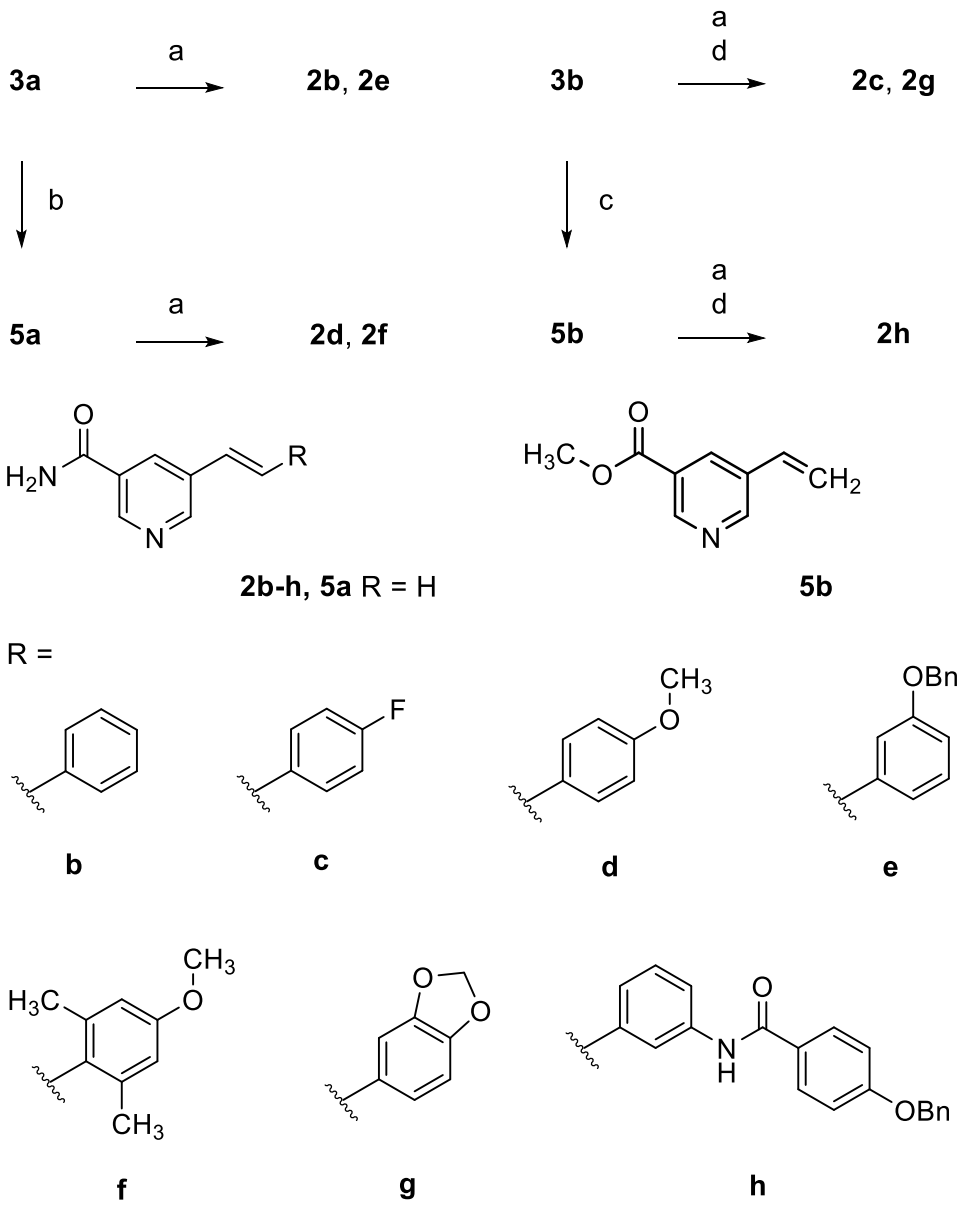

Scheme 2: Reagents and conditions: a) Pd_2dba_3 or $Pd(OAc)_2$, P(*o*-tol)$_3$, TEA, DMF, 120-140 °C, 0.7-24 h, 11-75 %; b) potassium vinyltrifluoroborate, Cs_2CO_3, $PdCl_2(PPh_3)_2$, ACN, H_2O, 1.5 h, 120 °C, 78 % c) tributylvinyl tin, $Pd(PPh_3)_4$; toluene, reflux, 3 h, 76 %; d) NH_3, MeOH, 40 °C, 3 d, 87-95 %.

Compounds **2b** and **2e** were obtained in moderate yield using **3a** as the arylhalide in the Heck reaction. The use of **3b** in the Heck reaction resulted in a substantial

improvement of yield in the synthesis of **2g** but not for **2c**. Interchanging the roles by using 5-vinylnicotinamide (**5a**) or methyl 5-vinylnicotinate (**5b**) as alkene component had detrimental effects on the yields in the synthesis of **2d**, **2f** and **2h**. Intermediates **5a** and **5b** were accessible from **3a** and **3b** via Suzuki-Miyaura or Stille coupling [20].

Biology

The influence on deacetylase activity of three human sirtuin isoforms (Sirt1–3) was determined in a fluorescence-based assay, using *Z*-Lys(Acetyl)-AMC (ZMAL) as a substrate [25]. Compared to the lead structure **2a**, all compounds except **2e**-**h** show increased inhibitory activity against Sirt2. Compound **2c** represents the most potent inhibitior with an IC_{50} value of about 7 µM. Moreover, a slight increase in selectivity for Sirt2 and Sirt3 over Sirt1 could be observed for **2c**, **4a** and **4b**. While none of the modifications provided complete isoenzyme specificity, **2c** preferentially inhibited Sirt2 (IC_{50} 6.6 ± 0.5) and Sirt3 (IC_{50} 7.5 ± 0.9 µM) compared to Sirt1 (51 % inhibition at 100 µM). Interestingly, for compounds **4a** and **b**, this increase in selectivity results from increased rigidity of the C,C-double bond. A fluorescence polarization (FP)-based assay, localised binding of **2b** and **c** outside the selectivity pocket of Sirt2 [21].

Table 1: Sirt1–3 inhibition for compounds **2a-h** and **4a** and **b**

Entry	Sirt1 inhibition[a]	Sirt2 inhibition[a]	Sirt3 inhibition[a]
2a	27 % @ 50 µM	24.6 ± 2.8 µM [b]	41.7 ± 2.0 µM [b]
2b	71 % @ 10 µM	8.7 ± 0.2 µM [b]	89 % @ 50 µM

2c	51 % @ 100 µM	6.6 ± 0.5 µM [b]	7.5 ± 0.9 µM [b]
2d	51 % @ 10 µM	64 % @ 10 µM	90 % @ 50 µM
2e	61 % @ 50 µM	69 % @ 50 µM	60 % @ 50 µM
2f	26 % @ 10 µM	21 % @ 10 µM	79 % @ 50 µM
2g	52 % @ 50 µM	62 % @ 50 µM	87 % @ 50 µM
2h	n.i.	8.9 % @ 10 µM	n.i.
4a	n.i.	48 % @ 10 µM	38 % @ 10 µM
4b	n.i.	45 % @ 10 µM	38 % @ 10 µM

[a] Percent inhibition relative to controls at the indicated concentration, n.i. = no inhibition detected. [b] IC_{50} values (µM) with statistical limits; values are the mean±SD of duplicate experiments.

Photochemistry of Stilbenes

The photochemical behaviour of stilbenes has been subject to intense investigation in the past. It is reported that unsubstituted stilbene undergoes *E*→*Z* photoisomerization [26], as well as photocyclization to dihydrophenanthrene upon UV irradiation, which is oxidized to phenantrene in the presence of oxygen [27]. In high concentrations, (*E*)-stilbene furthermore undergoes photocyclodimerization to cyclobutane derivatives [28]. Photoisomerization and photocyclization are also reported for 3-styrylpyridines,

forming two regioisomeric dihydroazaphenanthrenes that are oxidized to 2- and 4-azaphenantrene (not shown), respectively [29].

Photochemistry of stilbenes **2b** and **2f** was analysed via UV/Vis-spectroscopy and LC/HR-MS. Upon exposure of a solution of **2b** in methanol to UV-A, changes in the UV/Vis-spectra proceeded relatively slow, due to the low absorbance of **2b** in this wavelength region. However, UV-B radiation revealed fast and dramatic changes, which increased with the length of irradiation. The initial spectrum did not restore, neither thermally by standing in the dark nor photochemically, when exposed to daylight.

LC/HR-MS indicated the generation of three different species as products of the photochemical reaction of a 10 mM solution of **2b** in methanol when exposed to 5 minutes of UV irradiation. Besides the two isomers *E*-**2b** and *Z*-**2b** generated by photoisomerization, two major fractions were detected, that could represent different isomers of benzoquinoline carboxamides **8a** and **b** formed by photocyclization and oxidation (Scheme 3).

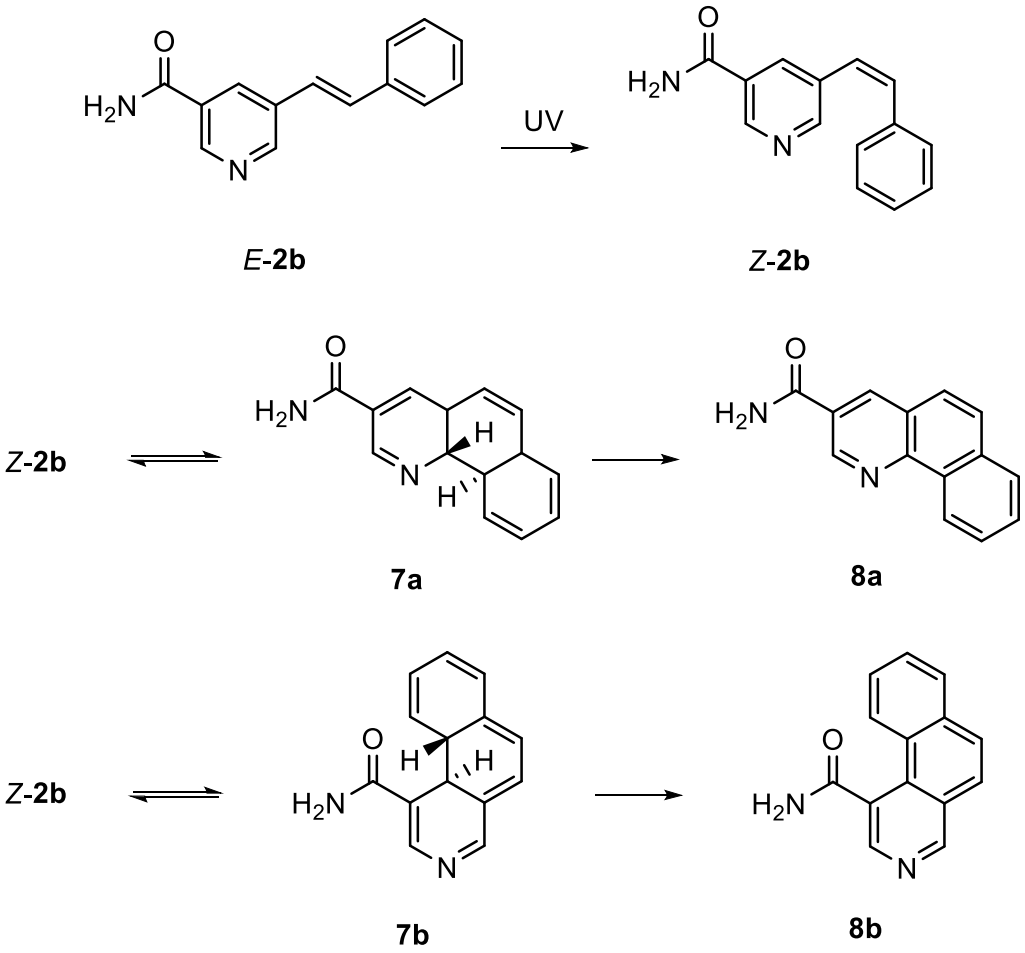

Scheme 3: Photocyclization and oxidation reaction of **2b** upon UV-B irradiation.

As a third species, cycloaddition products in two fractions were found. If a 100 µM methanolic solution of **2b** was irradiated with UV radiation, cycloaddition products could not be identified so that this reaction seems only to take place in highly concentrated solutions.

To verify the hypothetical structures, we carried out quantum chemical calculations of the double bond isomers *E*-**2b** and *Z*-**2b** as well as the oxidized compounds **8a** and **8b**. We used Density Functional Theory (DFT) to optimize the ground state equilibrium

structures of *E*-**2b**, *Z*-**2b**, **8a** and **8b**, and used time-dependent DFT (TDDFT) and high-level correlated methods to obtain UV/Vis absorption energies and oscillator strengths. To obtain the simulated absorption spectrum and λ_{max} values, oscillator strengths were converted into molar decadic extinction coefficients using a Gaussian line shape with a full-width-at-half-maximum of 0.3 eV. The correlated methods used were second-order approximated coupled cluster singles and doubles (CC2) and its approximation, algebraic diagrammatic construction to second-order (ADC(2)) [30–32]. ADC2 calculations have also been carried out with the implicit solvent continuum model COSMO using a dielectricity constant and refractive index of an methanol/water mixture, which was used as solvent in the experimental UV/Vis measurements of the LC/HR-MS fractions [33, 34]. Geometries for reactants ***E*-2b** and ***Z*-2b** were optimized for two different rotational isomers (***E*-2b-A** and ***E*-2b-B**; ***Z*-2b-A** and ***Z*-2b-B**), defined in the Supporting Information. In the following, we report only the results for ***E*-2b-B** and ***Z*-2b-A**, since they possess lower ground state energies and therefore are expected to be the dominant species at room temperature. Energy differences of the ground state structures of two pairs of isomers, however, are less than 0.6 kcal/mol, and computed spectra differ only slightly. Extensive results of all structures and all applied computational methods are summarized in the Supporting Information.

While TDDFT systematically underestimates the λ_{max} values of the lowest absorption of all compounds by 0.1-0.75 eV, CC2 and ADC(2) agree with the λ_{max} values of the lowest absorption bands with a maximum deviation of 0.15 eV, similar to the previously determined accuracy [35]. We notice a good agreement between ADC(2) gas phase calculations with CC2 gas phase calculations, which justifies the usage of the

approximate ADC(2) method. Comparing the calculated absorption spectra for ***E*-2b-B** and ***Z*-2b-A** to the experimental spectra obtained from LC/HR-MS (Figure 3, A, B), we see that all calculations consistently confirm the experimentally found blue shift of about 15 nm (0.22 eV) for the λ_{max} value of the lowest absorption band. Blue shifts predicted by CC2, ADC(2), ADC(2)/COSMO are 14, 16, and 20 nm, respectively. Consistent with the experimental spectra, all theoretical methods predict the maximum extinction of the lowest absorption band of ***Z*-2b** to approximately one half of the one of ***E*-2b**. Since the maximum error of the methods (0.15 eV) is smaller than the observed blue shift (0.22 eV), we conclude that the computed λ_{max} values are meaningful and clearly support the successful formation of the *Z*-isomer. Regarding the spectra of the photocyclization and oxidation products **8a** and **8b** (Figure 3, C, D), theoretical methods predict the λ_{max} value of the lowest absorption bands within 8 nm (~0.15 eV) of the value of the experimental spectrum of the LC/HR-MS, clearly confirming the experimentally found blue shift of 0.75 eV and 0.54 eV compared to compounds ***E*-2b** and ***Z*-2b**, respectively. Also here, we conclude that the calculations clearly support the formation of compounds **8a** and/or **8b**. However, due to the similarity of the spectra of **8a** and **8b**, calculations do not allow to predict which of the two isomers was present in the fraction analysed. Electronic structure calculations of two cycloaddition products (dimer I and dimer II) are depicted in the Supporting Information and support the experimentally found data qualitatively by strongly decreased extinction coefficients and blue shifted λ_{max} values.

If a 50 µM solution of **2f** in methanol was irradiated, 10 minutes of UV-A irradiation were sufficient to reach a persistent photostationary state (PSS), that was not altered

by further UV-A, UV-B or visible light irradiation, nor by standing several days in the dark at room temperature (Figure 2). LC/HR-MS analysis of an irradiated 10 mM methanolic solution of **2f** indicated only small traces of the cycloaddition product, as well as *E*-**2f** and *Z*-**2f**. No formation of benzoquinoline carboxamides was registered, due to the sterically blocking *ortho* methyl groups in **2f,** which prevented intramolecular photocyclization.

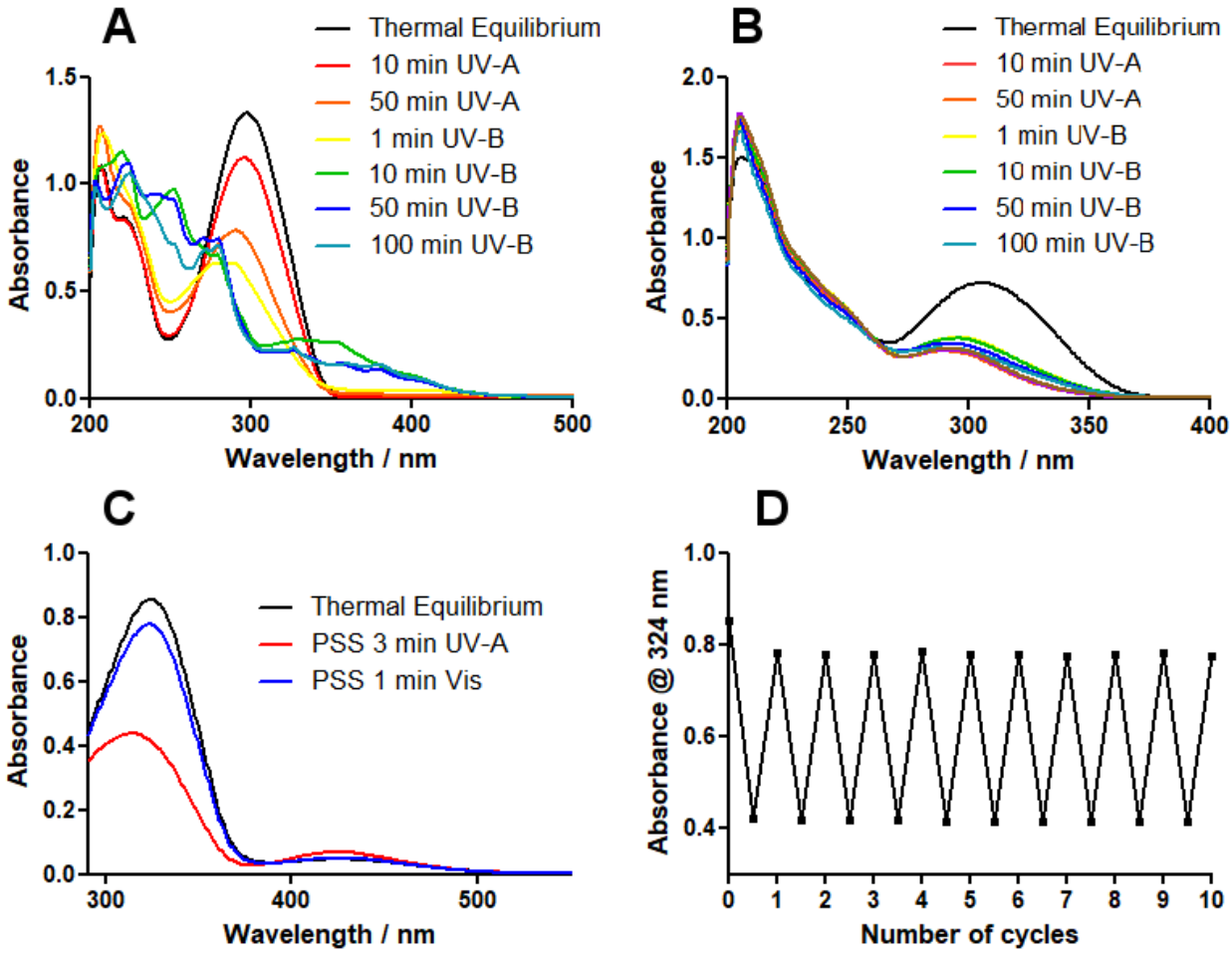

Figure 2: (A) UV/Vis spectrum of **2b** 50 µM in methanol after varying durations of UV radiation. (B) UV/Vis spectrum of **2f** 50 µM in methanol after varying durations of UV radiation. (C) UV/Vis spectrum of **11** 50 µM in 5 % DMSO in assay buffer at the thermal

equilibrium and the photostationary states (PSS) after UV-A or blue light radiation. (D) Fatigue resistance of **11** 50 µM in 5 % DMSO in assay buffer over 10 cycles of alternating UV-A and blue light radiation.

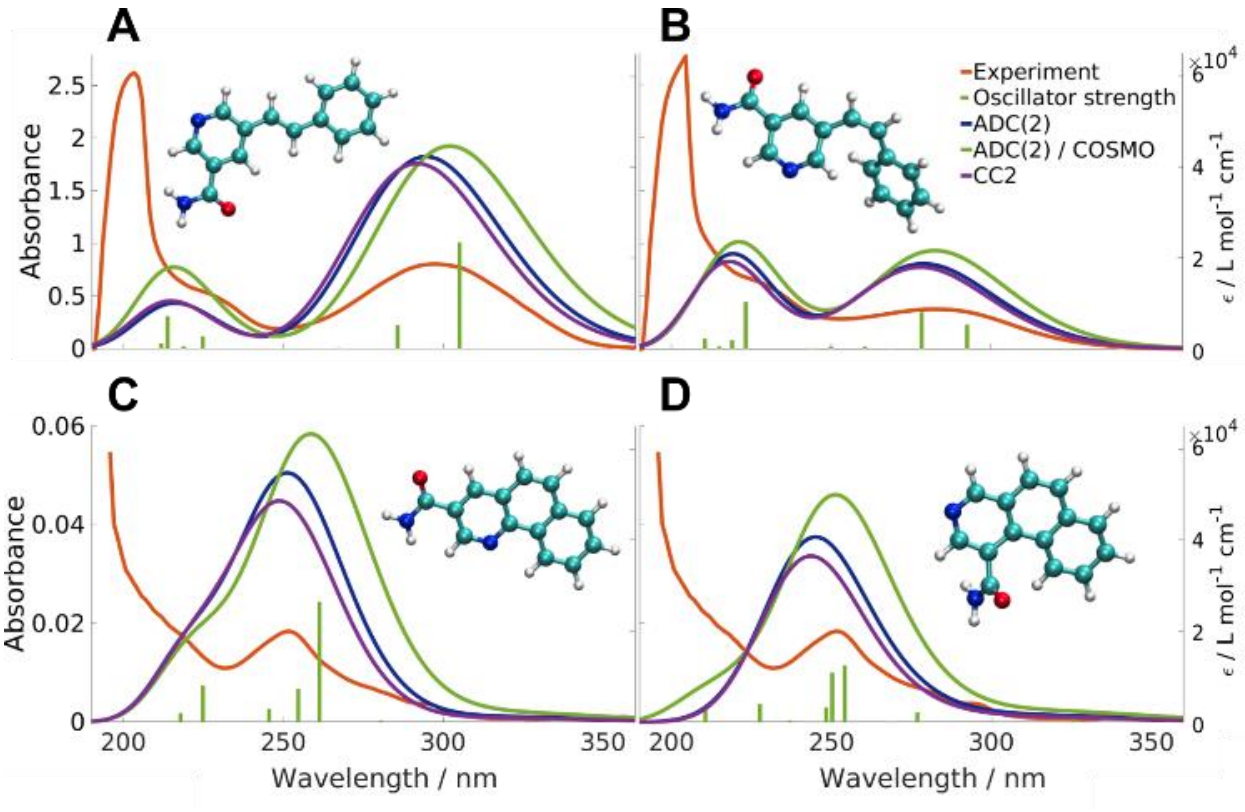

Figure 3: Calculated and experimental absorption spectra of compounds ***E*-2b-B** (A), ***Z*-2b-A** (B), and products **8a** (C) and **8b** (D). Oscillator strengths (green sticks) correspond to the ADC(2)/COSMO calculation.

Synthesis and Photochemistry of Photoswitchable Diazeno Analogue

Even though the photochemical properties of 2,6-dimethylstyryl nicotinamides like **2f** seemed promising with regard to the absence of photochemical side reactions in low concentrations, we envisioned to replace the stilbene motive of selected stilbene **2c** by

a diazeno group, because photoisomerization was anticipated to be reversible by application of UV-A irradiation and visible light, respectively in this analogue.

5-Diazenylnicotinamide **11** was synthetically accessible in two steps through conversion of commercially available methyl 5-aminonicotinate (**9**) and 4-flouroaniline to **10** under Mill's reaction conditions and subsequent ammonolysis of the methyl ester **10** to amide **11** (Scheme 4).

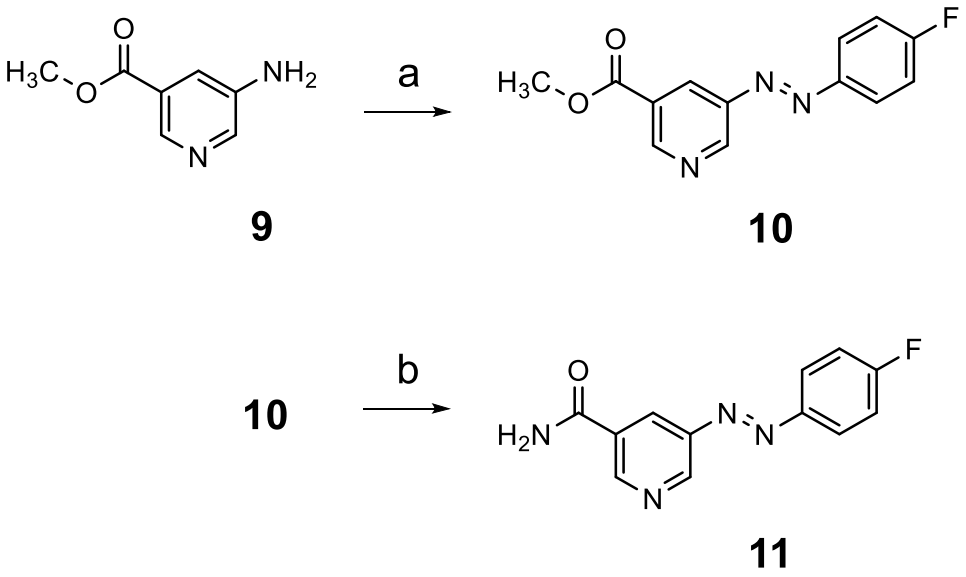

Scheme 4: Synthesis of diazeno compound **11**: a) 4-flouroaniline, oxone, HAc, 60 °C, 14 d, 42 %; b) NH_3, MeOH, RT, 3 d, 98 %.

Photoswitching of *E*-**11** to a long-living PSS ($t_{½}$ = 16 h) containing 84 % of *Z*-**11** was possible by short term UV-A irradiation. The photoisomerization could be reversed by exposure to visible light, i.e. blue light, albeit the PSS after blue light irradiation still comprised about 25 % of *Z*-**11** (Table 2) as determined by HPLC analysis using UV-Vis detection at the isosbestic points. Green light could also reverse

photoisomerization, but was not as effective as blue light. Ruby light, in contrast, did not lead to an altered PSS composition obtained by UV-A irradiation. Switching between the two PSS could be repeated several times without any observable fatigue of the compound (Figure 2).

Table 2: Percentage of *E*/*Z*-isomers of **11** at the thermal equilibrium (Δ), and photostationary states (PSS) after UV-A and blue light irradiation.

	Δ	PSS 5 min UV-A	PSS 1 min blue
E-**11**/*Z*-**11**	99 / 1	16 / 84	75 / 25

The photoswitchable diazeno compound **11** was subjected to biological evaluation to test the effect of photoisomerization on the inhibitory activity. The enzyme assay mixture containing **11** was exposed to 5 minutes of UV-A radiation and compared with the results of a non-irradiated measurement. The applied UV-A radiation did not perturb the proper enzyme functioning as proved by an unaltered enzyme activity in the blank tests. Unfortunately, UV-A radiation turned out to have only negligible effects on the IC_{50} values of **11** (Table 3).

Table 3. Sirt1-3 inhibition for compound **11** at the thermal equilibrium (Δ) and the photostationary state (PSS) after 5 min of UV-A irradiation.

Entry	Sirt1 inhibition[a]	Sirt2 inhibition[a]	Sirt3 inhibition[a]

Δ	n.i. @ 10 µM	18.9 ± 1.38 µM	27.5 ± 3.42 µM
PSS	n.i. @ 10 µM	24.1 ± 1.69 µM	29.9 ± 2.11 µM

[a] Percent inhibition relative to controls at the indicated concentration, n.i. = no inhibition detected.

Discussion

In recent years, photopharmacology has become a reputable strategy to optically control biochemical processes in the field of enzyme and ion channel modulation and recently 7TM-receptors also called GPCRs. Whereas in most approaches towards photoswitchable ligands the structure of the lead has to be changed considerable in order to incorporate a photoswitchable structural element, this was not the case with stilbene-based lead structure **2a**. Typically, it is not clear from the beginning, if the remodelling of the bioactive compounds will lead to an active diazeno derivative or not. The so-called azologization approach, moulded by Trauner et al., features a rational strategy for the design of photoswitchable compounds from established drug molecules through replacing certain core motives with an isosteric azobenzene moiety [36–38]. Recent examples have proven successful for receptor ligands by exchange of a linear alkinyl spacer for the zigzag shaped *E*-diazeno group [39]. In that instance, the geometry of the lead had to be changed considerably but careful design led to useful photoswitches. In the case of lead **2a** no such alteration of geometry was necessary and thus it seemed highly likely, that biological activity could be maintained. Indeed, this hypothesis could be proven. Exchange of the stilbene double-bond with a

diazeno bridge, caused only a slight decrease in inhibitory potency against Sirt2 and Sirt3, and the selectivity profile of diazeno compound **11** equals the profile of its direct stilbene analogue **2f**. The other part of the hypothesis was, that by photoinduced isomerization a considerable drop of activity would occur due to the conformational change and the resulting changed geometry and polarity. However, this part of our hypothesis turned out to be wrong. The over-all conformational changes upon photoisomerization were too small or did not lead to a hindered binding, as anticipated. This result is disappointing, because the photoswitchable sirtuin inhibitor **11** cannot be switched between active and inactive state, as envisioned. Possible reasons could be assigned to substituent effects as recently demonstrated by Simeth et al. [40]. Even if the change in space orientation does not alter binding, we would have predicted, that at least the difference in polarity of *E*-**11** and *Z*-**11** should lead to marked differences of sirtuin engagement in vitro. However, recent results from a carefully designed azologization study performed by Rustler et al. led to comparable difficulties [41].

Conclusions

Based on lead structure GW435821X (**2a**) a small library of analogous stilbene compounds was designed, synthesized and tested for their inhibitory activity against the human sirtuin isoforms Sirt1, Sirt2 and Sirt3. Compared to the lead structure inhibitory potency could be increased to single digit µM potency for some compounds, while isoenzyme selectivity still remains an issue. The photochemistry of stilbene compounds **2b** and **2f** was studied. For **2b**, besides photoisomerization, formation of benzoquinoline carboxamides by photocyclization and oxidation was indicated by high

accuracy mass spectroscopy. Theoretical UV/Vis spectra for ***E*-2b**, ***Z*-2b** and two isomeric benzoquinoline carboxamides reproduced the experimental data and support this assumption. **2f** was unsusceptible to photocyclization due to sterically blocking *ortho* methyl groups but could not be toggled between *E*- and *Z*-configuration. This lead to the synthesis of a first diazenyl derivative of the lead structure **2a** with promising photochemical characteristics for a new class of photoswitchable sirtuin inhibitors, but the activity difference for the *E*- and *Z*-isomers needs dramatic improvement before a useful molecular probe can be obtained by this approach.

Experimental Section

General Remarks

All solvents and reagents were obtained from commercial suppliers and were used without purification. Anhydrous solvents were purchased from Acros Organics. Thin layer chromatography (TLC) was executed on silica gel 60 F_{254} aluminium plates purchased from Merck. Visualization of the compounds was accomplished by UV-light (254 nm and 366 nm) and by staining with iodine, DNPH/H_2SO_4 (2 g 2,4-dinitrophenylhydrazine and 5 mL H_2SO_4 in 50 mL EtOH and 16 mL water) or vanillin/sulfuric acid (3.0 g vanillin and 0.5 mL H_2SO_4 in 100 mL EtOH) reagent. Synthesis was additionally monitored using high speed SFC/MS runs performed by a Nexera SFE-SFC/UHPLC switching system (Shimadzu Corporation, Kyoto, Japan) consisting of a pumping system (one LC-30ADSF for liquid CO_2 and two LC-20ADXR for modifier and make-up delivery), an on-line supercritical fluid extraction module

(SFE-30A auto extractor equipped with 0.2 mL extraction vessels) for reaction monitoring, an autosampler (SIL-30AC) for purified compounds, a column thermostat (CTO-20AC) equipped with a Torus DIOL (Waters) or Phenomenex CSP (Lux Amylose-2, i-Amylose-3, i-Cellulose-5), a degasser (DGU-20A5R), a communications module (CBM-20A), and two back pressure regulators BPR A and B (SFC-30A). UV and MS spectra were recorded via photodiode array detection (SPD-M20A) and electrospray ionization single quadrupole MS (LCMS-2020) controlled by Shimadzu LabSolution software (Version 5.91). Chromatographic purification of products was performed by flash chromatography on silica gel (20–45 µm, Carl Roth) applying pressured air up to 0.8 bar. NMR spectra were recorded on a Bruker Avance III instrument (^{1}H NMR: 400 MHz, ^{13}C NMR: 100.6 MHz). Chemical shifts were referenced to tetramethylsilane (TMS) as internal standard in deuterated solvents and reported in parts per million (ppm). Coupling constants (*J*) are reported in Hz using the abbreviations: s = singlet, d = doublet, t = triplet, q = quartet, m = multiplet and combinations thereof, br = broad. Infrared (IR-) spectra were recorded on a Bruker Alpha FT-IR spectrometer equipped with a diamond ATR unit and are indicated in terms of absorbance frequency [cm^{-1}]. Microwave synthesis was conducted in a Monowave 300 microwave synthesis reactor from Anton Paar equipped with appropriate sealed reaction vessels G10 (6 mL) or G30 (20 mL), applying a maximum initial power of 850 W to reach a given temperature (IR sensor) for a given time with stirring at 600 rpm. Melting points were measured in open capillary tubes using a Melting Point M-565 apparatus from Büchi and are uncorrected. High accuracy mass spectra were recorded on a Shimadzu LCMS-IT-TOF using ESI ionization. Purity of

final compounds was determined by HPLC with DAD (applying the 100 % method at 220 nm). Preparative and analytical HPLC were performed using Shimadzu devices CBM-20A, LC-20A P, SIL-20A, FRC-10A with SPD 20A UV/Vis detector and an ELSD-LTⅡ. In analytical mode a LiChroCART® (250×4 mm) and in preparative mode a Hibar® RT (250×25 mm) column, both containing LiChrospher® 100 RP-18e (5 µm), were used. An Elementar Vario MICRO cube was used for the experimental determination of elemental configurations of final pure products. UV/Vis-spectra were obtained using a Thermo Scientific Genesys 10S UV-VIS spectrophotometer.

Synthesis

General procedure for synthesis of nicotinamides from methyl nicotinates: The respective methyl nicotinate was treated with a saturated solution of ammonia in anhydrous MeOH (30 mL) and stirred in a sealed vessel at 40 °C until thin layer chromatography indicated complete conversion of the starting material. The solvent was evaporated under reduced pressure and the residue washed sparingly with cold MeOH.

(*E*)-5-Styrylnicotinamide (2b): In a microwave reaction vessel **3a** (1.01 g, 5.00 mmol, 1.00 equiv.) was mixed with styrene (651 mg, 6.25 mmol, 1.25 equiv.), tris(*o*-tolyl)phosphine (61 mg, 0.20 mmol, 0.04 equiv.), $Pd_2(dba)_3$ (92 mg, 0.10 mmol, 0.02 equiv.) and NEt_3 (863 µL, 0.63 g, 6.25 mmol, 1.25 equiv.) and suspended in anhydrous DMF (6 mL). The reaction was conducted at 120 °C for 40 min in a microwave reactor. After cooling to room temperature the mixture was taken up in EtOAc and filtered through a pad of Celite®. The filtrate was washed with water (3 x

30 mL) and sat. aq. NaCl-solution (30 mL), dried over $MgSO_4$ and concentrated under reduced pressure. The formed precipitate was collected by filtration and recrystallized from EtOAc. The product was obtained as colourless crystals (0.55 g, 2.45 mmol, 49 %): R_f = 0.25 (Cyclohexane/THF 1:1); mp: 196.4 °C; **^{1}H NMR (400 MHz, DMSO-*d*$_6$):** δ (ppm) = 8.93 (d, *J* = 2.0 Hz, 1H), 8.90 (d, *J* = 2.1 Hz, 1H), 8.50 (pseudo-t, *J* = 2.0 Hz, 1H), 8.24 (s, br, 1H), 7.71–7.62 (m, 3H), 7.54–7.28 (m, 5H); **^{13}C NMR, DEPT135, HSQC, HMBC (75.5 MHz, DMSO-*d*$_6$):** δ (ppm) = 166.4, 150.4, 147.3, 136.4, 132.4, 131.4, 131.3, 129.6, 128.7, 128.2, 126.7, 124.2; **IR (ATR):** *v* (cm^{-1}) = 3372, 3168, 1649, 1619, 1492, 1394, 961, 746, 691, 568; **ESI-HRMS:** calcd. for $[C_{14}H_{12}N_2O+H]^+$ 224.0950, found 224.0939; **Comp. Purity (220 nm):** 100 %; **Elem. Anal.:** calcd. for $C_{14}H_{12}N_2O$: N 12.49, C 74.98, H 5.39, found: N 12.38, C 74.81, H 5.15.

(*E*)-5-[3-(Benzyloxy)styryl]nicotinamide (2e): Synthesis was conducted according to the procedure of **2b** using **3a** (603 mg, 3.00 mmol, 1.00 equiv.), 1-(benzyloxy)-3-vinylbenzene (946 mg, 4.50 mmol, 1.50 equiv.), tris(*o*-tolyl)phosphine (91 mg, 0.30 mmol, 0.10 equiv.), $Pd(OAc)_2$ (34 mg, 0.15 mmol, 0.05 equiv.) and NEt_3 (1.25 mL, 913 mg, 9.00 mmol, 3.00 equiv.) in anhydrous DMF (4 mL). The reaction was conducted at 140 °C for 1.5 h in a microwave reactor. The raw product was recrystallized from ACN yielding a colourless solid (328 mg, 0.99 mmol, 33 %): R_f = 0.51 (EtOAc/MeOH 4:1); mp: 190.4 °C; **^{1}H NMR, H,H-COSY (400 MHz, DMSO-*d*$_6$):** δ (ppm) = 8.92 (s, 1H), 8.88 (s, 1H), 8.48 (s, 1H), 8.22 (s, br, 1H), 7.67 (s, br, 1H), 7.49 (d, *J* = 7.6 Hz, 2H), 7.46–7.38 (m, 4H), 7.37–7.27 (m, 3H), 7.23 (d, *J* = 7.4 Hz, 1H), 6.98 (d, *J* = 7.9 Hz, 1H), 5.17 (s, 2H); **^{13}C NMR, DEPT135, HSQC, HMBC (75.5 MHz,**

DMSO-*d*$_6$): δ (ppm) = 166.3, 158.7, 150.4, 147.3, 137.9, 137.0, 132.3, 131.4, 131.1, 129.8, 129.7, 128.4, 127.8, 127.7, 124.6, 119.6, 114.8, 112.5, 69.2; **IR (ATR):** *v* (cm^{-1}) = 3382, 3190, 1652, 1619, 1585, 1292, 1249, 1012, 965, 696; **ESI-HRMS:** calcd. for $[C_{21}H_{18}N_2O_2+H]^+$ 330.1368, found 330.1365; **Comp. Purity (220 nm):** 99.9 %; **Elem. Anal.:** calcd. for $C_{21}H_{18}N_2O_2$: N 8.48, C 76.34, H 5.49, found: N 8.35, C 75.89, H 5.19.

(*E*)-5-(4-Methoxystyryl)nicotinamide (2d): In an inert gas atmosphere 4-bromoanisole (468 mg, 2.50 mmol, 1.00 equiv.) was mixed with **5a** (407 mg, 2.75 mmol, 1.0 equiv.), Pd_2dba_3 (114 mg, 0.13 mmol, 0.05 equiv.) and tris(*o*-tolyl)phosphine (76 mg, 0.25 mmol, 0.10 equiv.) and suspended in anhydrous DMF (10 mL). After addition of NEt_3 (1.04 mL, 759 mg, 7.50 mmol, 3.00 equiv.) the reaction mixture was stirred at 120 °C for 24 h. The mixture was filtrated through a pad of Celite® and taken up in EtOAc (70 mL). The organic phase was washed with water (3 × 30 mL) and aq. sat. NaCl-solution (30 mL), then dried over $MgSO_4$. After evaporation of the solvent under reduced pressure, the residue was recrystallized from cyclohexane/EtOAc. The product was obtained as colourless solid (110 mg, 0.43 mmol, 17 %): R_f = 0.25 (DCM/MeOH 95:5); mp: 222.3 °C; **^{1}H NMR, H,H-COSY (400 MHz, DMSO-*d*$_6$):** 8.88 (d, *J* = 1.9 Hz, 1H), 8.84 (d, *J* = 1.9 Hz, 1H), 8.45–8.43 (m, 1H), 8.20 (s, br, 1H), 7.65 (s, br, 1H), 7.59 (d, 8.7 Hz, 1H), 7.42 (d, *J* = 16.5 Hz, 1H), 7.19 (d, *J* = 16.5 Hz, 1H), 6.99 (d, 8.7 Hz, 1H), 3.80 (s, 3H); **^{13}C NMR, DEPT135, HSQC, HMBC (75.5 MHz, DMSO-*d*$_6$):** 166.4, 159.4, 150.1, 146.8, 132.7, 131.0, 130.9, 129.6, 129.1, 128.1, 121.8, 114.2, 55.1; **IR (ATR):** *v* (cm^{-1}) = 3339, 2969, 1675, 1603, 1387, 1022, 953, 818, 696, 626; **ESI-HRMS:** calcd. for $[C_{15}H_{14}N_2O_2+H]^+$ 254.1055,

found 254.1056; **Comp. Purity (220 nm):** 100 %; **Elem. Anal.:** calcd. for $C_{15}H_{14}N_2O_2$: N 11.02, C 70.85, H 5.55, found: N 10.95, C 70.85, H 5.28.

(*E*)-5-(4-Methoxy-2,6-dimethylstyryl)nicotinamide (2f): Synthesis was conducted according to the procedure of **2d** using **5a** (593 mg, 2.76 mmol, 1.00 equiv.), 2-bromo-5-methoxy-1,3-dimethylbenzene (532 mg, 3.59 mmol, 1.30 equiv.), Pd_2dba_3 (128 mg, 0.14 mmol, 0.05 equiv.), tris(*o*-tolyl)phosphine (85 mg, 0.28 mmol, 0.10 equiv.) and NEt_3 (1.15 mL, 838 mg, 8.28 mmol, 3.00 equiv.) in anhydrous DMF (10 mL). The reaction was conducted at 120 °C for 3 h. The crude product was purified by silica gel column chromatography (EtOAc/MeOH 95:5), which yielded a colourless solid (88 mg, 0.31 mmol, 11 %): R_f = 0.39 (EtOAc/MeOH 95:5); mp: 188.3 °C; **^{1}H NMR, H,H-COSY (400 MHz, DMSO-*d*$_6$):** 8.90 (d, *J* = 2.0 Hz, 1H), 8.86 (d, *J* = 2.0 Hz, 1H) , 8.43 (pseudo-t, *J* = 2.0 Hz, 1H), 8.21 (s, br, 1H), 7.65 (s, br, 1H), 7.39 (d, *J* = 16.8 Hz, 1H), 6.72 (d, *J* = 17.4 Hz, 1H), 6.69 (s, 2H), 3.75 (s, 3H), 2.35 (s, 6H); **^{13}C NMR, DEPT135, HSQC, HMBC (75.5 MHz, DMSO-*d*$_6$):** 166.4, 157.8, 150.0, 147.1, 137.4, 132.7, 131.1, 129.6, 129.2, 128.5, 128.3, 113.4, 54.8, 21.1; **IR (ATR):** *v* (cm^{-1}) = 3171, 2958, 1670, 1598, 1383, 1308, 1299, 1145, 1064, 691; **ESI-HRMS:** calcd. for $[C_{17}H_{18}N_2O_2+H]^+$ 282.1368, found 282.1361; **Comp. Purity (220 nm):** 100 %; **Elem. Anal.:** calcd. for $C_{17}H_{18}N_2O_2$: N 9.92, C 72.32, H 6.41, found: N 9.61, C 71.77, H 6.61.

Methyl (*E*)-5-(4-fluorostyryl)nicotinate: Synthesis was conducted according to the procedure of **2b** using **3b** (648 mg, 3.00 mmol, 1.00 equiv.), 1-fluoro-4-vinylbenzene (550 mg, 4.50 mmol, 1.50 equiv.), tris(*o*-tolyl)phosphine (183 mg, 0.60 mmol, 0.20 equiv.), $Pd_2(dba)_3$ (67 mg, 0.30 mmol, 0.10 equiv.) and NEt_3 (1.25 mL, 9.00 mmol, 3.00 equiv.) in anhydrous DMF (4 mL). The reaction was conducted at

140 °C for 1.5 h. The raw product was purified by silica gel column chromatography (*n*-hexane/EtOAc 2:1) yielding a colourless solid (97 mg, 0.38 mmol, 13 %): R_f = 0.50 (*n*-hexane/EtOAc 2:1); mp: 108.2 °C; **^{1}H NMR, H,H-COSY (400 MHz, $CDCl_3$):** δ (ppm) = 9.09 (d, *J* = 1.8 Hz, 1H), 8.90 (d, *J* = 2.1 Hz, 1H), 8.52 (pseudo-t, *J* = 2.0 Hz, 1H), 7.57–7.49 (m, 2H), 7.26 (d, *J* = 16.4 Hz, 1H), 7.13–7.06 (m, 2H), 7.03 (d, *J* = 16.4 Hz, 1H); 4.00 (s, 3H, H-8); **^{13}C NMR, DEPT135, HSQC, HMBC (75.5 MHz, $CDCl_3$):** δ (ppm) = 165.3, 163.2 (d, *J* = 249.4 Hz), 150.1, 147.7, 135.0, 134.0, 135.7, 132.4 (d, *J* = 3.4 Hz), 132.2, 128.8 (d, *J* = 8.2 Hz), 126.9, 122.9 (d, *J* = 2.3 Hz), 116.2 (d, *J* = 21.8 Hz), 52.9; **IR (ATR):** *v* (cm^{-1}) = 2957, 1718, 1508, 1433, 1299, 1230, 986, 821, 763; **ESI-HRMS:** calcd. for $[C_{15}H_{12}NO_2F+H]^+$ 257.0852, found 257.0850.

(*E*)-5-(4-Fluorostyryl)nicotinamide (2c): Synthesis was conducted following the general procedure of nicotinamides from methyl nicotinates, using methyl (*E*)-5-(4-fluorostyryl)nicotinate (75 mg, 0.31 mmol, 1.00 equiv.). The product was obtained as colourless solid (65 mg, 0.27 mmol, 87 %): R_f = 0.48 (EtOAc/MeOH 95:5); mp: 205.6 °C; **^{1}H NMR, H,H-COSY (400 MHz, DMSO-*d*$_6$):** δ (ppm) = 8.91 (d, *J* = 1.9 Hz, 1H), 8.88 (d, *J* = 2.0 Hz, 1H), 8.47 (pseudo-t, *J* = 2.0 Hz, 1H), 8.22 (s, 1H), 7.76–7.68 (m, 2H), 7.49 (d, *J* = 16.6 Hz, 1H), 7.31 (d, *J* = 16.6 Hz, 1H), 7.29–7.22 (m, 2H); **^{13}C NMR, DEPT135, HSQC, HMBC (75.5 MHz, DMSO-*d*$_6$):** δ (ppm) = 166.4, 161.9, 150.3, 147.3, 133.1 (d, *J* = 3.2 Hz), 132.3, 131.4, 130.1, 129.7, 128.6 (d, *J* = 8.2 Hz), 124.1 (d, *J* = 2.2 Hz), 115.7 (d, *J* = 21.6 Hz); **IR (ATR):** *v* (cm^{-1}) = 3364, 3172, 1650, 1620, 1507, 1397, 1212, 968, 857, 601; **ESI-HRMS:** calcd. for $[C_{14}H_{11}N_2OF+H]^+$ 242.0855, found 242.0844; **Comp. Purity (220 nm):** 100 %; **Elem. Anal.:** calcd. for $C_{14}H_{11}N_2OF$: N 11.56, C 69.41, H 4.58, found: N 11.53, C 69.89, H 4.51.

5-(3,4-Dihydronaphthalen-2-yl)nicotinamide (4a): In a microwave reaction vessel **3a** (234 mg, 1.17 mmol, 1.00 equiv.), (3,4-dihydronaphthalen-2-yl)boronic acid (226 mg, 1.30 mmol, 1.11 equiv.) and $Pd(PPh_3)_4$ (75 mg, 0.065 mmol, 0.05 equiv.) were mixed together and suspended in DMF (2 mL). After addition of $NaHCO_3$ (328 mg, 3.90 mmol, 3.33 equiv.) in water (3 mL) the mixture was reacted at 150 °C for 15 min. After cooling to room temperature EtOAc (25 mL) and water (25 mL) were added and the catalyst removed by filtration through a pad of Celite®. The watery phase was extracted with EtOAc (3 x 10 mL) and the combined organic phases washed with water (3 x 20 mL) and sat. aq. NaCl-solution (25 mL), then dried over $MgSO_4$. After evaporation of the solvent the residue was recrystallized from acetone and obtained as colourless solid (125 mg, 0.50 mmol, 43 %): R_f = 0.36 (hexanes/Acetone 1:1); mp: 217.7 °C; **^{1}H NMR (400 MHz, DMSO-*d*$_6$):** δ (ppm) = 8.97 (d, *J* = 1.8 Hz, 1H), 8.93 (d, *J* = 1.5 Hz, 1H), 8.39 (pseudo-t, *J* = 2.1 Hz, 1H), 8.24 (s, br, 1H), 7.65 (s, br, 1H), 7.30–7.12 (m, 5H), 2.93 (t, *J* = 8.1 Hz, 1H), 2.76 (t, *J* = 8.1 Hz, 1H); **^{13}C NMR, DEPT135, HSQC, HMBC (75.5 MHz, DMSO-*d*$_6$):** δ (ppm) = 166.4, 148.4, 147.3, 135.2, 134.5, 134.5, 133.7, 131.0, 129.3, 127.6, 127.2, 126.9, 126.6, 125.9, 27.1, 24.9; **IR (ATR):** *v* (cm^{-1}) = 3363, 3193, 1672, 1623, 1397, 1140, 891, 778, 751, 610; **ESI-HRMS:** calcd. for $[C_{16}H_{14}N_2O+H]^+$ 250.1106, found 250.1097; **Comp. Purity (220 nm):** 100 %; **Elem. Anal.:** calcd. for $C_{16}H_{14}N_2O$: N 11.19, C 76.78, H 5.64, found: N 10.90, C 76.72, H 5.38.

5-(Naphthalen-2-yl)nicotinamide (4b): Synthesis was conducted according to the procedure of **4a** using **3a** (100 mg, 0.50 mmol, 1.00 equiv.), naphthalen-2-ylboronic acid (112 mg, 0.65 mmol, 1.30 equiv.), $Pd(PPh_3)_4$ (29 mg, 0.025 mmol, 0.05 equiv.) in

DMF (3 mL), together with $NaHCO_3$ (126 mg, 1.50 mmol, 3.00 equiv.) in water (2 mL). The reaction was conducted at 150 °C for 15 min in a microwave reactor. The product was obtained as colourless crystals (79 mg, 0.32 mmol, 64 %): R_f = 0.37 (Hexanes/Acetone 1:1); mp: 217.7 °C; **^{1}H NMR (400 MHz, $CDCl_3$):** δ (ppm) = 9.19 (d, *J* = 2.2 Hz, 1H), 9.06 (d, *J* = 2.0 Hz, 1H), 8.64 (pseudo-t, *J* = 2.1 Hz, 1H), 8.40 (d, *J* = 1.0 H, 1H), 8.32 (s, br, 1H), 8.08 (d, *J* = 8.6 Hz, 1H), 8.06–8.01 (m, 1H),7.65 (s, br, 1H), 7.30–7.12 (m, 5H), 2.93 (t, *J* = 8.1 Hz, 1H), 2.76 (t, *J* = 8.1 Hz, 1H); **^{13}C NMR, DEPT135, HSQC, HMBC (75.5 MHz, $CDCl_3$):** δ (ppm) = 166.4, 150.1, 147.7, 134.9, 133.7, 133.2, 133.1, 132.6, 129.7, 128.8, 128.3, 127.6, 126.7, 126.5, 124.8; **IR (ATR):** *v* (cm^{-1}) = 3385, 3190, 1686, 1397, 1144, 1129, 822, 775, 700, 479; **ESI-HRMS:** calcd. for $[C_{16}H_{12}N_2O+H]^+$ 248.0950, found 248.0943; **Comp. Purity (220 nm):** 100 %; **Elem. Anal.:** calcd. for $C_{16}H_{16}N_2O$: N 11.28, C 77.40, H 4.87, found: N 11.20, C 77.29, H 4.68.

Methyl 5-[(4-fluorophenyl)diazenyl]nicotinate (10): 4-Fluoroaniline (444 mg, 4.00 mmol, 1.00 equiv.) was dissolved in DCM (15 mL) and treated with a solution of oxone (4.92 g, 8.00 mmol, 2.00 equiv.) in water (50 mL). The biphasic mixture was vigorously stirred until thin layer chromatography indicated complete consumption of the starting material. The watery phase was discarded and the organic phase washed with an aq. HCl-solution (1M, 3 × 10 mL) and water (3 × 10 mL), then dried over $MgSO_4$. The solution was concentrated to a volume of 5 mL under reduced pressure and added to a solution of **9** (609 mg, 4.00 mmol, 1.00 equiv.) in acetic acid (20 mL). The reaction mixture was stirred at 60 °C for two weeks, cooled to room temperature, poured onto ice cooled sat. aq. $NaHCO_3$-solution and extracted with EtOAc (3 ×

50 mL). The combined organic extracts were washed with water (3 × 50 mL), sat. aq. NaCl-solution (30 mL) and dired over $MgSO_4$. The solvent was evaporated under reduced pressure and the residue purified by silica gel column chromatography (cyclohexane/EtOAc 3:1). The product was obtained as orange solid (431 mg, 1.67 mmol, 42 %): R_f = 0.52 (cyclohexane/EtOAc 3:1); mp: 103.6 °C; **^{1}H NMR, H,H-COSY (400 MHz, DMSO-*d*$_6$):** δ (ppm) = 9.34 (d, *J* = 2.3 Hz, 1H), 9.22 (d, *J* = 2.0 Hz, 1H), 8.50 (pseudo-t, *J* = 2.2 Hz, 1H), 8.09–8.01 (m, 2H), 7.52–7.44 (m, 2H), 3.95 (s, 3H); **^{13}C NMR, DEPT135, HSQC, HMBC (75.5 MHz, DMSO-*d*$_6$):** δ (ppm) = 164.5, 164.4 (d, *J* = 251.8 Hz), 151.8, 150.3, 148.5 (d, J = 2.8 Hz), 146.7, 126.4 (d, *J* = 6.7 Hz), 125.4 (d, *J* = 9.5 Hz), 116.6 (d, J = 23.2 Hz), 52.7; **IR (ATR):** *v* (cm^{-1}) = 3081, 1713, 1583, 1496, 1286, 1222, 1092, 1000, 843, 498.

5-[(4-Fluorophenyl)diazenyl]nicotinamide (11): Synthesis was conducted following the general procedure of nicotinamides from methyl nicotinates, using **10** (160 mg, 0.62 mmol, 1.00 equiv.). The product was obtained as orange solid (149 mg, 0.61 mmol, 98 %): R_f = 0.65 (EtOAc/MeOH 95:5); mp: 212.3 °C; **^{1}H NMR, H,H-COSY (400 MHz, DMSO-*d*$_6$):** δ (ppm) = 9.24 (d, *J* = 2.3 Hz, 1H), 9.20 (d, *J* = 2.0 Hz, 1H), 8.58 (pseudo-t, *J* = 2.2 Hz, 1H), 8.38 (s, br, 1H), 8.08–8.02 (m, 2H), 7.80 (s, br, 1H), 7.53–7.45 (m, 2H); **^{13}C NMR, DEPT135, HSQC, HMBC (75.5 MHz, DMSO-*d*$_6$):** δ (ppm) = 165.6, 164.3 (d, *J* = 251.4 Hz), 150.7, 148.6 (d, *J* = 2.8 Hz), 148.2, 146.7, 130.5, 125.7, 125.3 (d, *J* = 9.4 Hz), 116.6 (d, *J* = 23.2 Hz); **IR (ATR):** *v* (cm^{-1}) = 3359, 3125, 1669, 1628, 1496, 1398, 1136, 838, 808, 692; **ESI-HRMS:** calcd. for $[C_{12}H_9N_4OF+H]^+$ 224.0760, found 224.0753; **Comp. Purity (220 nm):** 100 %; **Elem. Anal.:** calcd. for $C_{12}H_9N_4OF$: N 22.94, C 59.02, H 3.71, found: N 22.95, C 59.46, H 3.92.

Bioassay: The inhibitory effect of compounds **2a**-**h**, **4a** and **b**, and **11** on Sirt1–3 was detected via a previously reported fluorescence based assay [25]. The synthetic substrate *Z*-Lys(Acetyl)-AMC (ZMAL) is deacetylated by sirtuins, followed by tryptic digestion and thereby release of 7-aminomethylcumarin, leading to a fluorescent readout. All compounds were tested at 100 µM, 50 µM and 10 µM respectively. For compounds that showed more than 50 % inhibition at 10 µM an IC_{50} value was determined. Inhibition measurements were performed in biological duplicates for all compounds.

Photochemistry: All photoisomerization experiments were conducted under ruby light. Illumination was executed using a Bio-Link 254 Crosslinker from Vilber-Lourmat equipped with six Ushio G8T5E lamps for UV-B (8W, 306 nm) or six Vilber-Lourmat T8-L lamps for UV-A (8W, 365 nm) radiation, respectively. Visible (red, green and blue) light irradiation was derived from a Paulmann FlexLED 3D strip. All compounds were irradiated in solution, using spectrophotometric grade solvents. Photoisomerization and UV/Vis-spectra measurement was conducted in quartz cuvettes at room temperature.

Computational Details: All calculations were carried out using the TURBOMOLE version 7.2 quantum chemistry package [42]. Geometry optimization of all compounds in different conformers were carried out using DFT with PBE approximation to the exchange-correlation (XC) functional and employ the SV(P) basis set [43, 44]. The 10 lowest excitation energies and their oscillator strengths were computed using the SV(P) basis and the larger def2-TZVP basis set [44]. This was done using TDDFT with the hybrid approximation to the XC functional PBE0, CC2, and ADC(2) [45, 30–32, 46,

47]. ADC(2) and CC2 calculations make use of the resolution-of-identity approximation [48]. ADC(2) calculations were also done using the continuum solvent model COSMO as previously described [33, 34, 49–51]. A dielectric constant of 62.14 and a refractive index of 1.3379 were used, which corresponds to a solvent of a 6/4-mixture of methanol/water, as experimentally determined [52, 53]. Broadened absorption spectra were simulated by converting oscillator strengths to decadic extinction coefficients using a Gaussian line shape with a full-width-at-half-maximum of 0.3 eV [54–57].

Supporting Information

The Supporting Information features experimental and analytical data for the synthesis of intermediates and compounds **2g** and **2h** as well as ^{1}H and ^{13}C NMR spectra for all synthesized compounds. Procedures of photochemical experiments and their analysis are described. Additionally, detailed summaries of electronic structure calculations for two conformers (A and B) of each double bond isomer (***E*-2b** and ***Z*-2b**), photocyclization and oxidation products **8a** and **8b** and two cycloaddition products are given.

Supporting Information File 1:

File Name: Supp1

File Format: .docx

Title: Experimental procedures, analytical data and quantum chemical calulations

Acknowledgements

The Jung group thanks the Deutsche Forschungsgemeinschaft (DFG, Ju295/14-1 and RTG1976) for funding.

References

1. Schiedel, M.; Robaa, D.; Rumpf, T.; Sippl, W.; Jung, M. *Med. Res. Rev.* **2018,** *38*, 147–200.
2. Frye, R. A. *Biochem. Biophys. Res. Commun.* **2000,** *273*, 793–798.
3. Vaziri, H.; Dessain, S. K.; Ng Eaton, E.; Imai, S. I.; Frye, R. A.; Pandita, T. K.; Guarente, L.; Weinberg, R. A. *Cell* **2001,** *107*, 149–159.
4. Perrod, S.; Cockell, M. M.; Laroche, T.; Renauld, H.; Ducrest, A. L.; Bonnard, C.; Gasser, S. M. *EMBO J.* **2001,** *20*, 197–209.
5. Tanno, M.; Sakamoto, J.; Miura, T.; Shimamoto, K.; Horio, Y. *J. Biol. Chem.* **2007,** *282*, 6823–6832.
6. Rumpf, T.; Schiedel, M.; Karaman, B.; Roessler, C.; North, B. J.; Lehotzky, A.; Oláh, J.; Ladwein, K. I.; Schmidtkunz, K.; Gajer, M.; Pannek, M.; Steegborn, C.; Sinclair, D. A.; Gerhardt, S.; Ovádi, J.; Schutkowski, M.; Sippl, W.; Einsle, O.; Jung, M. *Nat. Commun.* **2015,** *6*, 6263.
7. North, B. J.; Verdin, E. *PloS one* **2007,** *2* (8), e784.
8. Schwer, B.; North, B. J.; Frye, R. A.; Ott, M.; Verdin, E. *J. Cell Biol.* **2002,** *158*, 647–657.
9. AOP Orphan Pharmaceuticals AG, **2017,** Available at https://www.aoporphan.com/global_en/our-company/newsroom/aop-orphan-pharmaceuticals-ag-to-acquire-selisistat-a-clinical-stage-drug-candidate-for-the-treatment-of-huntingtons-disease-hd (Accessed June 17, 2019).
10. Süssmuth, S. D.; Haider, S.; Landwehrmeyer, G. B.; Farmer, R.; Frost, C.; Tripepi, G.; Andersen, C. A.; Di Bacco, M.; Lamanna, C.; Diodato, E.; Massai, L.; Diamanti, D.; Mori, E.; Magnoni, L.; Dreyhaupt, J.; Schiefele, K.; Craufurd, D.; Saft, C.; Rudzinska, M.; Ryglewicz, D.; Orth, M.; Brzozy, S.; Baran, A.; Pollio, G.; Andre, R.; Tabrizi, S. J.; Darpo, B.; Westerberg, G. *Br. J. Clin. Pharmacol.* **2015,** *79*, 465–476.
11. Chopra, V.; Quinti, L.; Kim, J.; Vollor, L.; Narayanan, K. L.; Edgerly, C.; Cipicchio, P. M.; Lauver, M. A.; Choi, S. H.; Silverman, R. B.; Ferrante, R. J.; Hersch, S.; Kazantsev, A. G. *Cell Rep.* **2012,** *2*, 1492–1497.

12. Outeiro, T. F.; Kontopoulos, E.; Altmann, S. M.; Kufareva, I.; Strathearn, K. E.; Amore, A. M.; Volk, C. B.; Maxwell, M. M.; Rochet, J.-C.; McLean, P. J.; Young, A. B.; Abagyan, R.; Feany, M. B.; Hyman, B. T.; Kazantsev, A. G. *Science* **2007,** *317*, 516–519.
13. Pillai, V. B.; Bindu, S.; Sharp, W.; Fang, Y. H.; Kim, G.; Gupta, M.; Samant, S.; Gupta, M. P. *Am. J. Physiol. Heart Circ. Physiol.* **2016,** *310*, H962-72.
14. Lu, Y.; Wang, Y.-D.; Wang, X.-Y.; Chen, H.; Cai, Z.-J.; Xiang, M.-X. *Int. J. Cardiol.* **2016,** *220*, 700–705.
15. He, X.; Zeng, H.; Chen, J.-X. *Int. J. Cardiol.* **2016,** *215*, 349–357.
16. Bellizzi, D.; Rose, G.; Cavalcante, P.; Covello, G.; Dato, S.; Rango, F. de; Greco, V.; Maggiolini, M.; Feraco, E.; Mari, V.; Franceschi, C.; Passarino, G.; Benedictis, G. *Genomics* **2005,** *85*, 258–263.
17. Longo, V. D.; Kennedy, B. K. *Cell* **2006,** *126*, 257–268.
18. Trapp, J.; Jochum, A.; Meier, R.; Saunders, L.; Marshall, B.; Kunick, C.; Verdin, E.; Goekjian, P.; Sippl, W.; Jung, M. *J. Med. Chem.* **2006,** *49*, 7307–7316.
19. Falenczyk, C.; Schiedel, M.; Karaman, B.; Rumpf, T.; Kuzmanovic, N.; Grøtli, M.; Sippl, W.; Jung, M.; König, B. *Chem. Sci.* **2014,** *5*, 4794–4799.
20. McDonald, O.; Lackey, K.; Davis-Ward, R.; Wood, E.; Samano, V.; Maloney, P.; Deanda, F.; Hunter, R. *Bioorg. Med. Chem. Lett.* **2006,** *16*, 5378–5383.
21. Swyter, S.; Schiedel, M.; Monaldi, D.; Szunyogh, S.; Lehotzky, A.; Rumpf, T.; Ovádi, J.; Sippl, W.; Jung, M. *Philos. Trans. R. Soc. Lond. B Biol. Sci.* **2018,** *373*.
22. Szymański, W.; Beierle, J. M.; Kistemaker, H. A. V.; Velema, W. A.; Feringa, B. L. *Chem. Rev.* **2013,** *113*, 6114–6178.
23. Buettelmann, B.; Alanine, A.; Bourson, A.; Gill, R.; Heitz, M.-P.; Mutel, V.; Pinard, E.; Trube, G.; Wyler, R. *CHIMIA* **2004,** *58*, 630–633.
24. Heck, R. F. *Palladium reagents in organic syntheses*, Academic Press: London, 1990.
25. Heltweg, B.; Trapp, J.; Jung, M. *Methods* **2005,** *36*, 332–337.
26. Smakula, A. *Z. Phys. Chem.* **1934,** *25B* (1).
27. Buckles, R. E. *J. Am. Chem. Soc.* **1955,** *77*, 1040–1041.
28. Ciamician, G.; Silber, P. *Ber. Dtsch. Chem. Ges.* **1902,** *35*, 4128–4131.

29. Lewis, F. D.; Kalgutkar, R. S.; Yang, J.-S. *J. Am. Chem. Soc.* **2001,** *123*, 3878–3884.
30. Christiansen, O.; Koch, H.; Jørgensen, P. *Chem. Phys. Lett.* **1995,** *243*, 409–418.
31. Hättig, C.; Köhn, A. *J. Chem. Phys.* **2002**, *117*, 6939–6951.
32. Hättig, C. *Adv. Quantum Chem.*, **2005**, 37–60.
33. Klamt, A.; Schüürmann, G. *J. Chem. Soc., Perkin Trans. 2* **1993,** 799–805.
34. Lunkenheimer, B.; Köhn, A. *J. Chem. Theory Comput.* **2013,** *9*, 977–994.
35. Send, R.; Kühn, M.; Furche, F. *J. Chem. Theory Comput.* **2011,** *7*, 2376–2386.
36. Broichhagen, J.; Frank, J. A.; c. *Acc. Chem. Res.* **2015,** *48*, 1947–1960.
37. Schoenberger, M.; Damijonaitis, A.; Zhang, Z.; Nagel, D.; Trauner, D. *ACS Chem. Neurosci.* **2014,** *5*, 514–518.
38. Morstein, J.; Awale, M.; Reymond, J.-L.; Trauner, D. *ACS Cent. Sci.* **2019**.
39. Hauwert, N. J.; Mocking, T. A. M.; Da Costa Pereira, D.; Lion, K.; Huppelschoten, Y.; Vischer, H. F.; Esch, I. J. P. de; Wijtmans, M.; Leurs, R. *Angew. Chem. Int. Ed.* **2019,** *58*, 4531–4535.
40. Simeth, N. A.; Bellisario, A.; Crespi, S; Fagnoni, M.; König, B. *J. Org. Chem.*, **2019,** *84*, 6565–6575.
41. Rustler, K.; Maleeva, G.; Bregestovski, P.; König, B. *Beilstein J. Org. Chem.* **2019,** *15*, 780–788.
42. TURBOMOLE V7.2 2017, a development of University of Karlsruhe and Forschungszentrum Karlsruhe GmbH, 1989-2007, TURBOMOLE GmbH, since 2007; available from http://www.turbomole.com..
43. Perdew; Burke; Ernzerhof. *Phys. Rev. Lett.* **1996,** *77*, 3865–3868.
44. Schäfer, A.; Horn, H.; Ahlrichs, R. *J. Chem. Phys.* **1992,** *97*, 2571–2577.
45. Perdew, J. P.; Ernzerhof, M.; Burke, K. *J. Chem. Phys.* **1996,** *105*, 9982–9985.
46. Bauernschmitt, R.; Ahlrichs, R. *Chem. Phys. Lett.* **1996,** *256*, 454–464.
47. Furche, F.; Ahlrichs, R. *J. Chem. Phys.* **2002,** *117*, 7433–7447.
48. Eichkorn, K.; Weigend, F.; Treutler, O.; Ahlrichs, R. *Theor. Chem. Acc.* **1997,** *97*, 119–124.
49. Haan, D. O. de; Tapavicza, E.; Riva, M.; Cui, T.; Surratt, J. D.; Smith, A. C.; Jordan, M.-C.; Nilakantan, S.; Almodovar, M.; Stewart, T. N.; Loera, A. de; Haan,

A. C. de; Cazaunau, M.; Gratien, A.; Pangui, E.; Doussin, J.-F. *Environ. Sci. Technol.* **2018,** *52*, 4061–4071.

50. Thompson, T.; Tapavicza, E. *J. Phys. Chem. Lett.* **2018,** *9*, 4758–4764.
51. Tapavicza, E.; Thompson, T.; Redd, K.; Kim, D. *Phys. Chem. Chem. Phys.* **2018,** *20*, 24807–24820.
52. Mashimo, S.; Kuwabara, S.; Yagihara, S.; Higasi, K. *J. Chem. Phys.* **1989,** *90*, 3292–3294.
53. Herráez, J. v.; Belda, R. *J. Solution Chem.* **2006,** *35*, 1315–1328.
54. Epstein, S. A.; Tapavicza, E.; Furche, F.; Nizkorodov, S. A. *Atmos. Chem. Phys.* **2013,** *13*, 9461–9477.
55. Schalk, O.; Geng, T.; Thompson, T.; Baluyot, N.; Thomas, R. D.; Tapavicza, E.; Hansson, T. *J. Phys. Chem.* **2016,** *120*, 2320–2329.
56. Cisneros, C.; Thompson, T.; Baluyot, N.; Smith, A. C.; Tapavicza, E. *Phys. Chem. Chem. Phys.* **2017,** *19*, 5763–5777.
57. Tapavicza, E.; Furche, F.; Sundholm, D. *J. Chem. Theory Comput.* **2016,** *12*, 5058–5066.